

van Velzen, E., Thieser, T., Berendonk, T., Weitere, M. and Gaedke, U. 2018. Inducible defense destabilizes predator–prey dynamics: the importance of multiple predators. – *Oikos* doi: 10.1111/oik.04868

## Appendix 1

### Comparison of exchange rates

While predator-avoidant and fitness-dependent exchange are very similar conceptually, they are not identical. To compare the temporal dynamics of exchange rates of these two scenarios, we simulated the ecological dynamics with a small amount of non-adaptive exchange ( $\chi_{\max} = 10^{-2}$ ). Based on these dynamics and Eq. 2 and 6 we then calculated how the resulting exchange rates under the predator-avoidant and fitness-dependent scenarios.

The simulations show that the maximum and minimum exchange rates are nearly identical; however, at low prey biomass, fitness-dependent exchange rates are distinctly higher than predator-avoidant exchange rates, especially when predator biomass is high at the same time (Fig. A1). Conversely, when prey biomass is high, fitness-dependent exchange is somewhat lower than predator-avoidant exchange (Fig. A1). This corresponds to the high per capita predation risk at low prey biomass generated by the predators' type II functional response (Fig. A1, Peacor 2003, Tollrian et al. 2015).

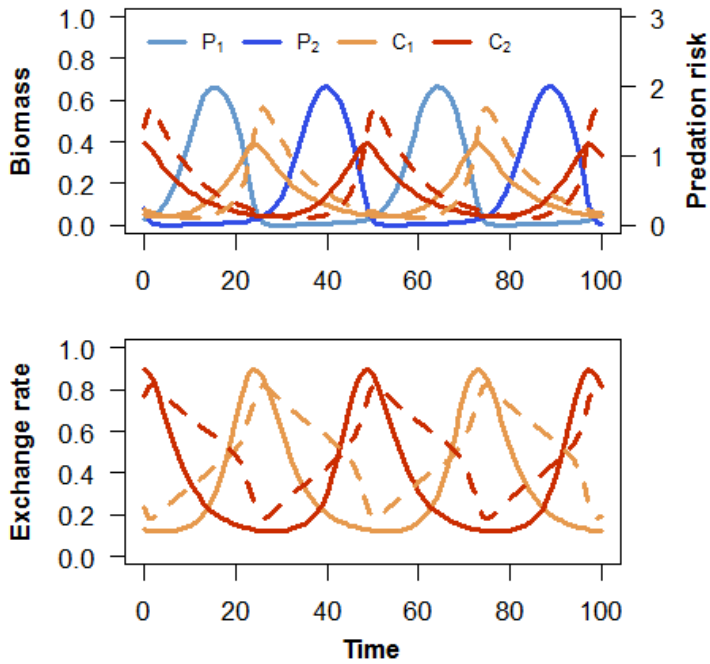


Figure A1. Comparison between predator-avoidant and fitness-dependent exchange rates. Upper panel: dynamics of predators and prey phenotypes (solid lines), using non-adaptive exchange;  $\chi_{\max} = 10^{-2}$ , for other parameters, Table 1. Dashed lines show per capita predation risk: predation of  $P_1$  by  $C_1$  (orange line) and predation of  $P_2$  by  $C_2$  (red line). Lower panel: exchange rates  $\chi_{12}$  (orange) and  $\chi_{21}$  (red) as fractions of  $\chi_{\max}$ . Solid lines: exchange rates under predator-avoidant exchange; dashed lines: exchange rates under fitness-dependent exchange.

## References

- Peacor, S. D. 2003. Phenotypic modifications to conspecific density arising from predation risk assessment. – *Oikos* 100: 409–415.
- Tollrian, R. et al. 2015. Density-dependent adjustment of inducible defenses. – *Sci. Rep.* 5: 12736.

## Appendix 2

### Supporting figures

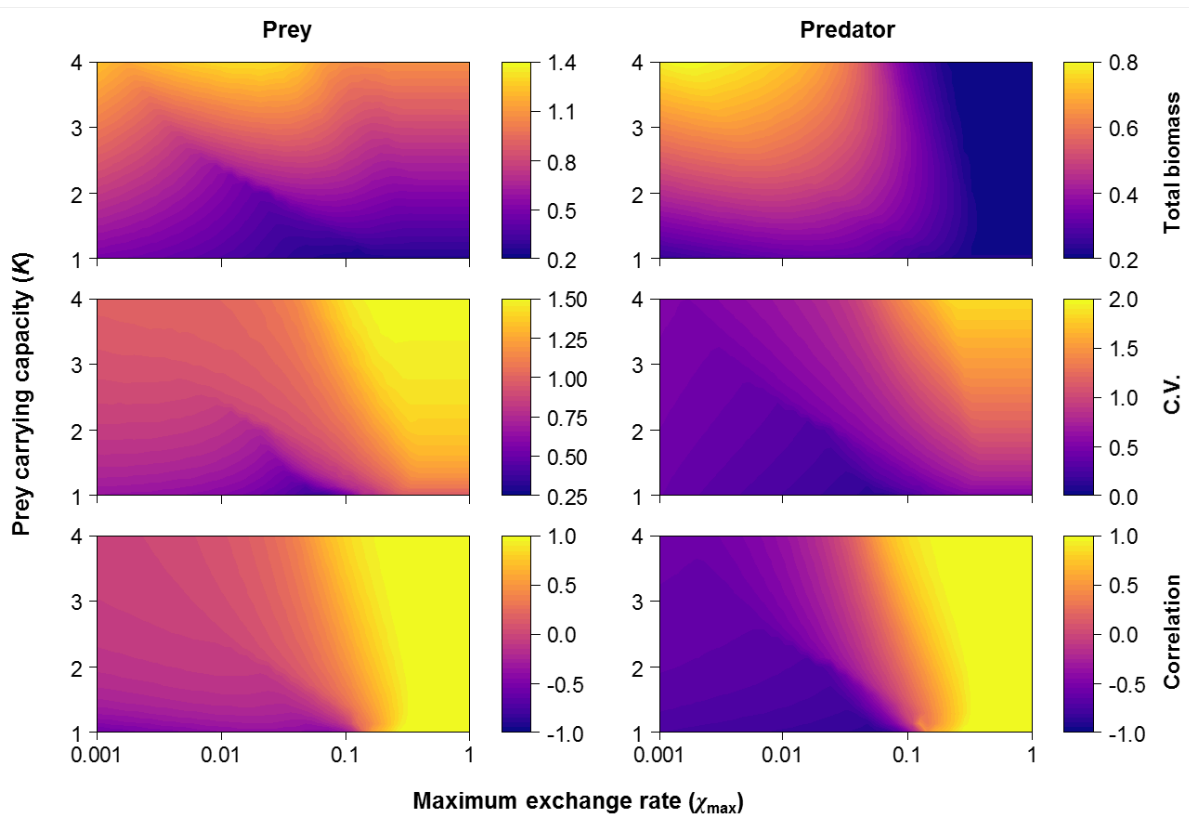


Figure A2.1. Impact of predator-avoidant exchange between prey phenotypes on total prey and total predator biomass (top), variability in the total biomass on both trophic levels (middle), and synchronization between the dynamics of the two phenotypes on both trophic levels (bottom).  $\alpha = 10$ , corresponding to an intermediate steepness (see Fig. 2a in the main text); all other parameter values can be found in Table 1. All patterns seen here strongly resemble those of the non-adaptive (diffusive) exchange model (cf. Fig. 5 and Results in main text).

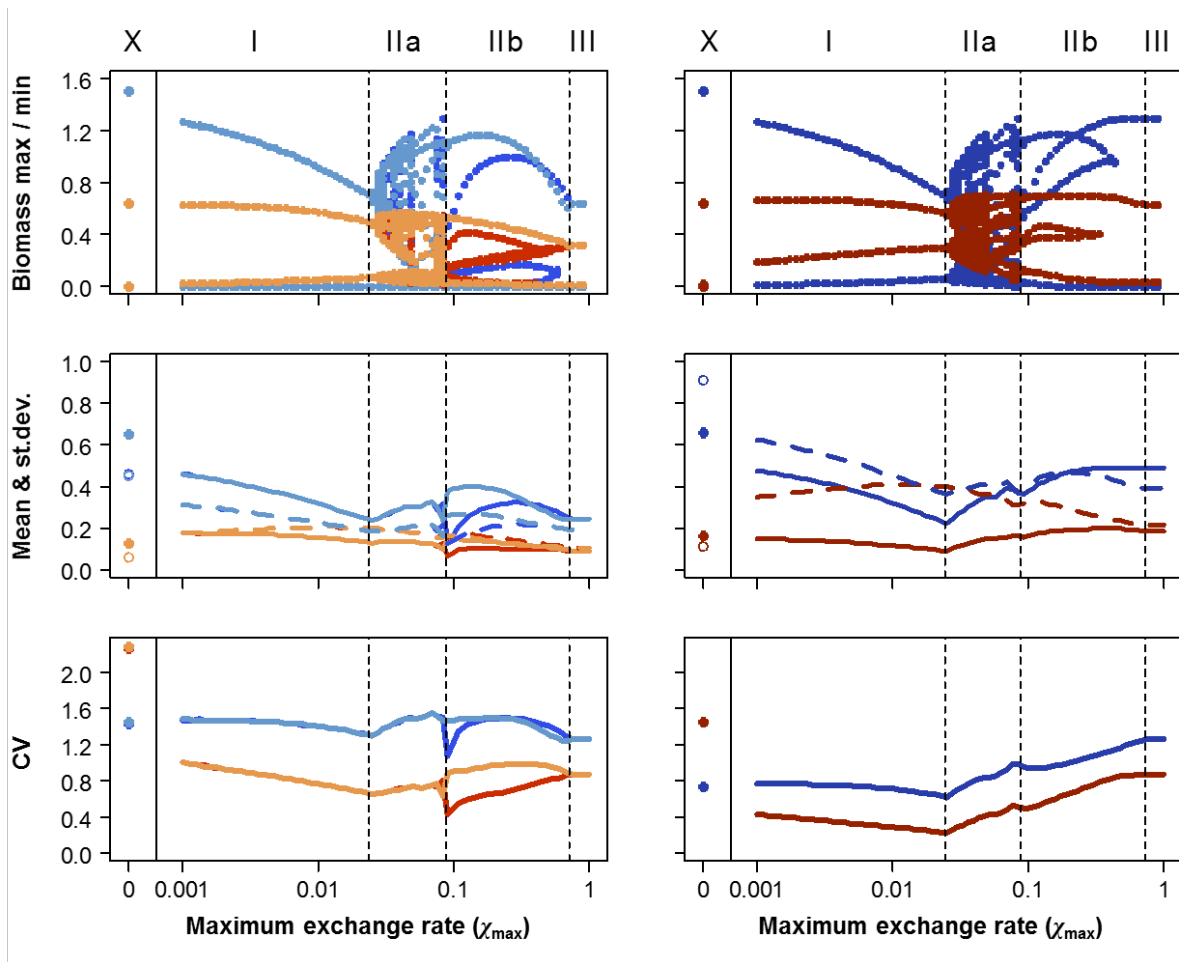


Figure A2.2. Bifurcation plots of the predator–prey dynamics (top panels) and the resulting mean biomasses, standard deviations and coefficients of variation of the dynamics (middle and bottom panels) for predator-avoidant exchange.  $K = 1.5$ ; other parameters the same as in Fig. B1. Top panels: maxima and minima of biomass dynamics. Middle panels: mean biomass (dashed lines in regions I–III; open symbols in region X) and standard deviations of the dynamics (solid lines in regions I–III; filled symbols in region X). Lower panels: CV (standard deviation divided by the mean). Left panels show the dynamics of individual prey phenotypes (blue) and predators (orange) are shown; right panels the dynamics of total prey (dark blue) and total predators (dark red). Exchange between prey phenotypes here results in four types of dynamics are found under nonzero exchange rates: symmetric compensatory dynamics (region I); chaotic dynamics (region IIa; see Fig. 8a in main text); regular complex oscillations (region IIb; see Fig. 8b in main text); and synchronized dynamics (region III).

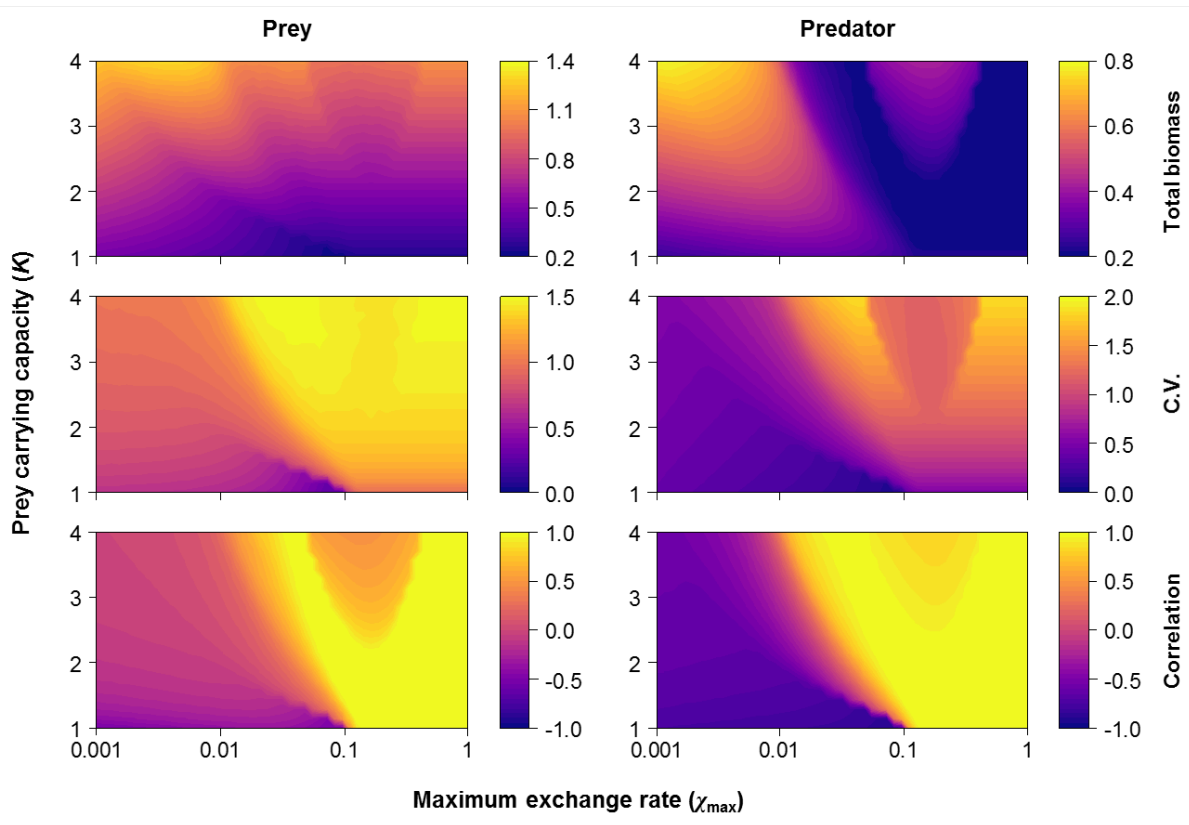


Figure A2.3. Impact of fitness-dependent exchange on total prey and total predator biomass (top), variability in the total biomass on both trophic levels (middle), and synchronization between the dynamics of the two phenotypes on both trophic levels (bottom).  $\theta = 1$ ; all other parameter values can be found in Table 1. All patterns strongly resemble those of the other two exchange scenarios (cf. Fig. 5, Fig. B1).

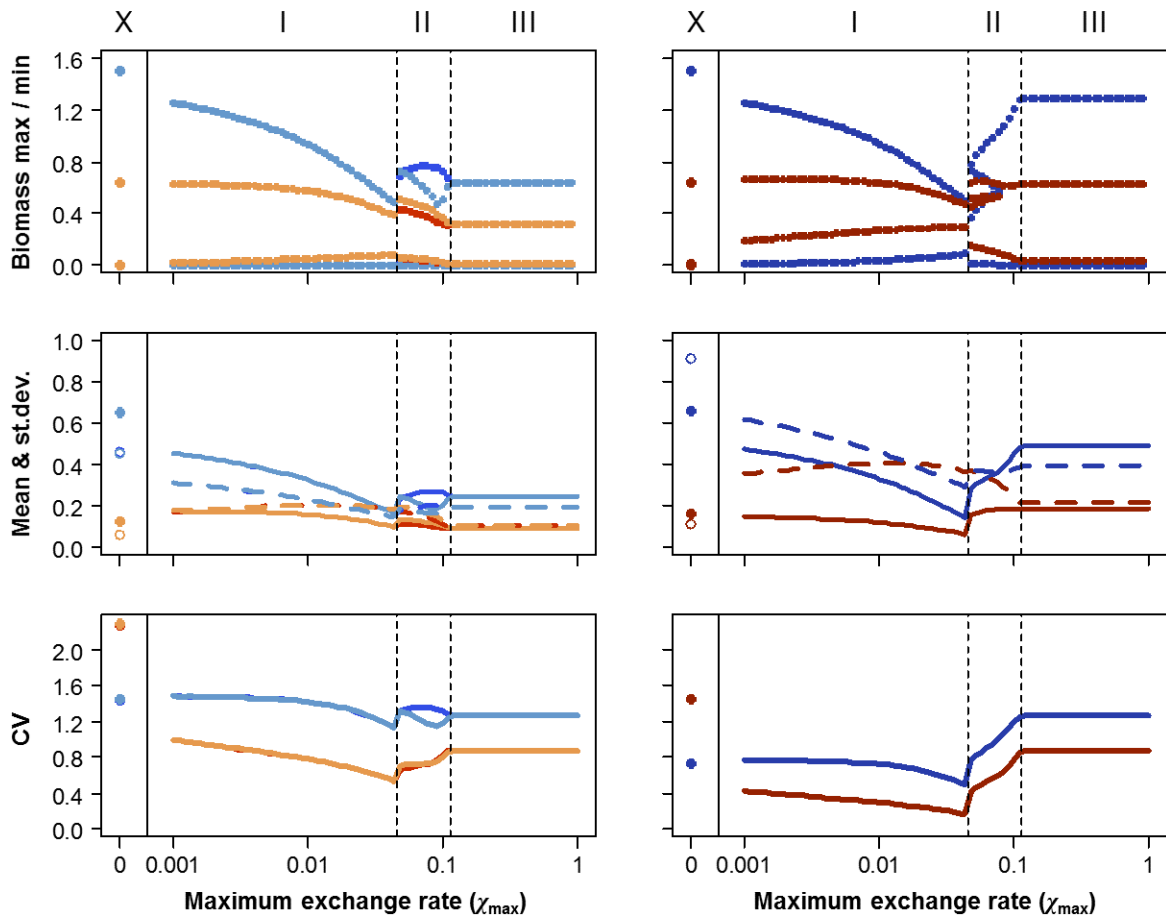


Figure A2.4. Bifurcation plots of the predator–prey dynamics, mean biomasses and standard deviations, and coefficients of variation (CV) of the dynamics under fitness-dependent exchange, with a fairly smooth response function ( $\theta = 2$ , see Fig. 2 in main text). All other parameters are the same as in Fig. 7 in the main text. Colours, lines and symbols have the same meaning as in Fig. B2. Exchange between prey phenotypes results in the same three types of dynamics as the non-adaptive exchange scenario (Fig. 4): symmetric compensatory dynamics (region I); asymmetric compensatory dynamics (region II); and synchronized dynamics (region III).

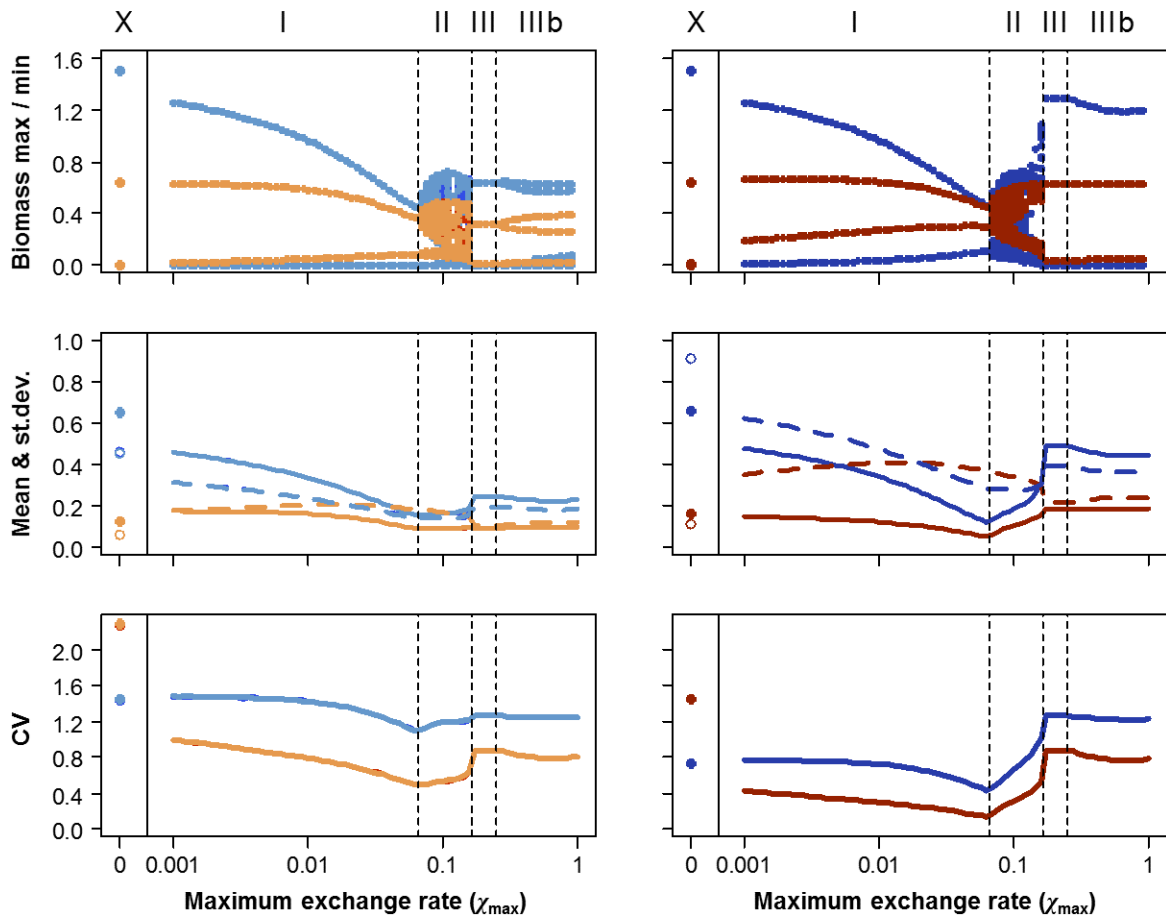


Figure A2.5. Bifurcation plots of the predator–prey dynamics, mean biomasses and standard deviations, and coefficients of variation (CV) of the dynamics under fitness-dependent exchange with a steep response function ( $\theta = 4.5$ , see Fig. 2 in main text). All other parameters are the same as in Fig. 7 in the main text. Colours, lines and symbols have the same meaning as in Fig. B2. Exchange between prey phenotypes here results in four types of dynamics: symmetric compensatory dynamics (region I); chaotic dynamics (region II); completely synchronized dynamics (region III); and asymmetric synchronized dynamics (region IIIb; see Fig. 8c in main text).

## Appendix 3

### Imperfect defense

In the model described in Eq. 1 in the main text, we assume predators are completely specialized, i.e. each prey phenotype is completely defended against one of the predators. Here we describe and analyze an extended model with some degree of niche overlap: each predator feeds mainly on its preferred prey, but it can feed to some extent on its non-preferred prey as well. This model is described by the following equations:

$$\begin{aligned}\frac{dP_i}{dt} &= r \left( 1 - \frac{P_1 + P_2}{K} \right) P_i - \chi_{ij} P_i + \chi_{ji} P_j - \frac{aP_i C_i}{1 + h(aP_i + c \cdot aP_j)} - \frac{caP_i C_j}{1 + h(caP_i + aP_j)} \\ \frac{dC_i}{dt} &= \left( \frac{\varepsilon(aP_i + caP_j)}{1 + h(aP_i + caP_j)} - d \right) C_i\end{aligned}\tag{A3.1}$$

where  $c$  is the degree of niche overlap between the two predators; all other parameters are the same as in the standard model and can be found in Table 1. We varied the degree of niche overlap from 0 – 15% in all three exchange scenarios (Fig. A3.1–A3.3) and found identical results. A higher degree of niche overlap (i.e. higher  $c$ ) increases consumer coupling; as a result, less exchange is necessary to synchronize prey dynamics (Fig. A3.1–A3.3, lower panels). Synchronized dynamics in turn result in low predator biomass and high variability in both prey and predator dynamics (Fig. A3.1–A3.3, top right and middle panels).

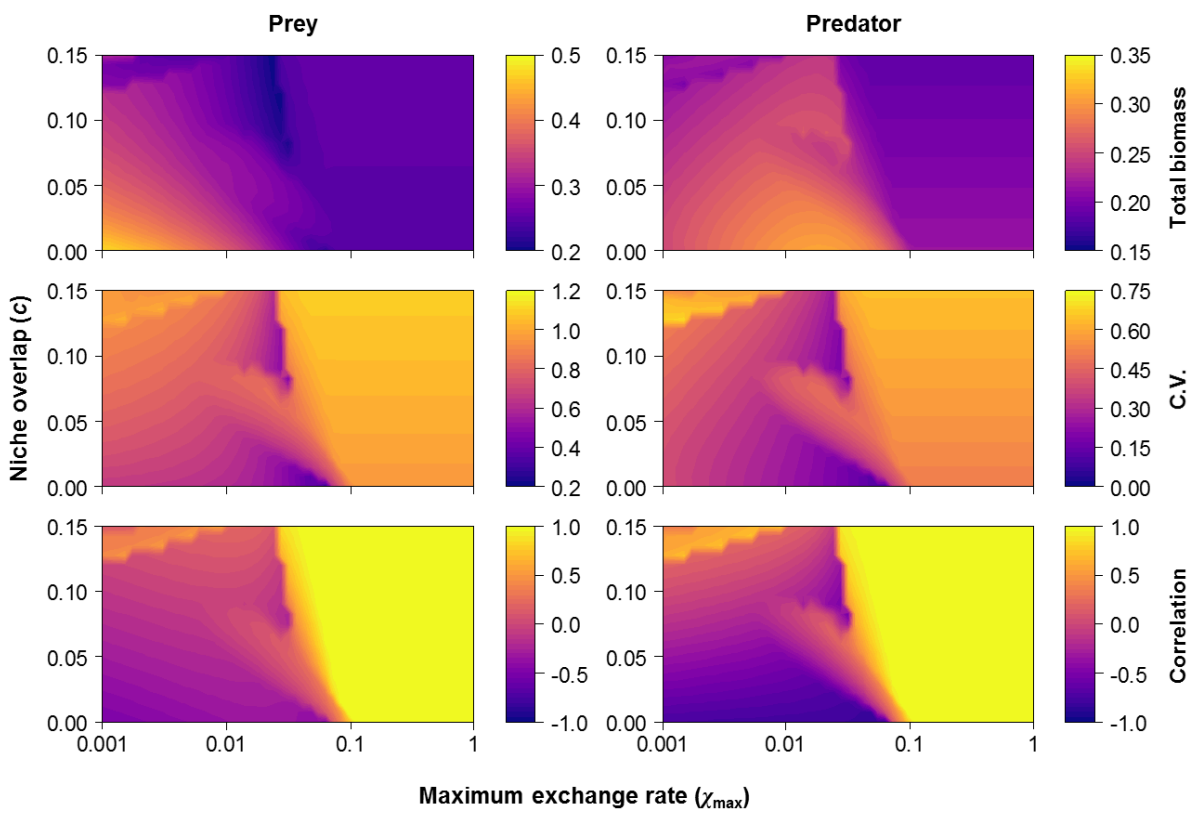


Figure A3.1. Impact of increasing niche overlap ( $c$ , Eq. A3.1) in the non-adaptive exchange scenario. Effect on total prey and total predator biomass (top), on variability in the total biomass on both trophic levels measured by the coefficient of variation (middle), and on synchronization between the two phenotypes on both trophic levels (bottom).  $K = 1$ ; for other parameter values, Table 1.

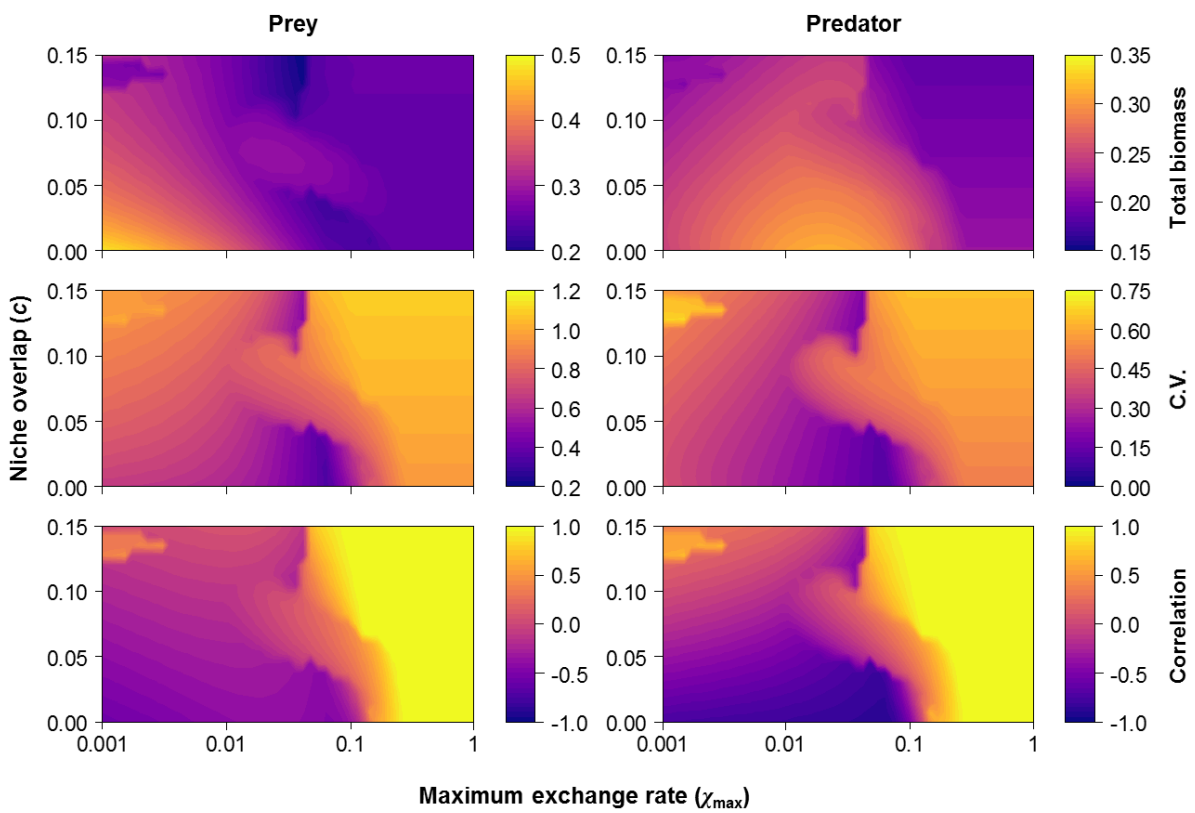


Figure A3.2. Impact of increasing niche overlap ( $c$ , Eq. A3.1) in the predator-avoidant exchange scenario. Effect on total prey and total predator biomass (top), on variability in the total biomass on both trophic levels measured by the coefficient of variation (middle), and on synchronization between the two phenotypes on both trophic levels (bottom).  $K = 1$ ,  $\alpha = 5$ ; for other parameter values, Table 1.

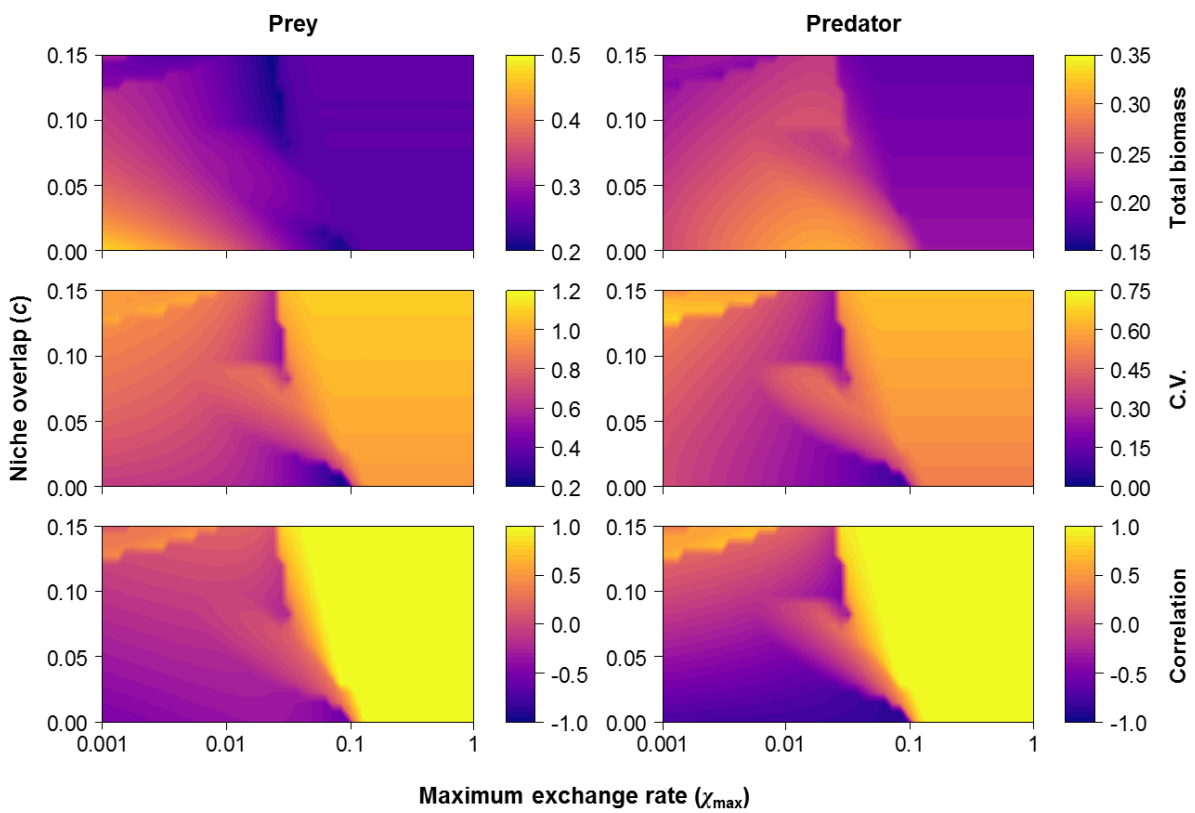


Figure A3.3. Impact of increasing niche overlap ( $c$ , Eq. A3.1) in the fitness-dependent exchange scenario. Effect on total prey and total predator biomass (top), on variability in the total biomass on both trophic levels measured by the coefficient of variation (middle), and on synchronization between the two phenotypes on both trophic levels (bottom).  $K = 1$ ,  $\theta = 1$ ; for other parameter values, Table 1.